J. Fluid Mech. (2007), *vol.* 592, *pp.* 195–220.
doi:10.1017/S0022112007008361 Printed in the United Kingdom

Trapped edge waves in stratified rotating fluids: numerical and asymptotic results

ALEXANDER T. I. ADAMOU[1], R. V. CRASTER[1] AND STEFAN G. LLEWELLYN SMITH[2]

[1]Department of Mathematics, Imperial College London, South Kensington Campus, London SW7 2AZ, UK

[2]Department of Mechanical and Aerospace Engineering, Jacobs School of Engineering, UCSD, La Jolla CA 92093-0411, USA

(Received 28 February 2007 and in revised form 31 July 2007)

The existence of trapped edge waves in a rotating stratified fluid with non-constant topography is studied using asymptotic and numerical techniques. A refinement of the classical WKBJ method is employed that is uniform at both the shoreline and caustic, where the classical approximation is singular, and is also uniform over long distances from the shore. This approach requires the use of comparison equations and it is shown that the two used previously in the literature are asymptotically equivalent in terms of the wave amplitude, but have small differences in the predicted wave frequencies. These asymptotic results, and results using shallow-water theory, are then compared to results from a careful numerical study of the nonlinear differential eigenvalue problem, allowing their range of practical applicability to be assessed. This numerical approach is also used to investigate whether trapping occurs in non-trivial and realistic geometries in the internal gravity wave band, which has been an open question for some time.

1. Background

Trapped modes are a feature of many physical systems that support waves: they arise in acoustics (Davies & Parnovski 1998; Adamou, Gridin & Craster 2005) and mathematically equivalent water wave problems (Evans, Levitin & Vassiliev 1994; McIver 1999), elasticity (Gridin, Craster & Adamou 2005*b*; Gridin, Adamou & Craster 2005*a*; Kaplunov, Rogerson & Tovstik 2005), and even as bound states in quantum waveguides (Duclos & Exner 1995; Linton & Ratcliffe 2004; Gridin, Adamou & Craster 2004). Another notable example of trapping is that of edge waves in physical oceanography. Edge waves propagate parallel to the shore and are confined to a certain distance from it, so that the trapping occurs in a direction transverse to the direction of propagation.

The existence of trapped waves in a homogeneous fluid over a sloping bottom has been known since the work of Stokes (1846). Stokes' edge wave was shown to be the gravest member of a family of modes by Ursell (1952). The Stokes wave always exists, while the number of higher modes is determined by the slope of the topography. There has been a considerable amount of work on edge waves in a homogeneous fluid, and recent extensions have considered the effect of surface tension (Muzylev, Bulgakov & Duran-Matute 2005), their generation (Evans 1988), nonlinear generalisations, and so on. Other generalisations of edge waves are on

the one hand to more general topography, and on the other hand to more realistic oceanographic situations in which both rotation and stratification play a role. For topography, Miles (1989), Zhevandrov (1991) and others have examined edge waves over a gently sloping bottom using asymptotic methods, but there does not appear to have been any numerical solution of this general edge wave problem. Greenspan (1970) added stratification, and Saint-Guily (1968) and Ou (1980) examined the effect of rotation on waves in a wedge. Rotation breaks the symmetry of the problem so that the waves propagating with the coast on their left are different from those with the coast on their right, as is the case for Kelvin waves (Pedlosky 1987). Evans (1989), Muzylev & Odulo (1980) and Llewellyn Smith (2004) – the last two independently – looked at the full problem. Llewellyn Smith notably summarized all the previous analyses and acts as a starting point for the current study.

An interesting alternative simplification is to apply a shallow-water approximation from the outset. This approach was used by Ball (1967) to investigate exponential topography and was subsequently expanded upon by Munk, Snodgrass & Wimbush (1970). We shall compare results with Ball's analysis where applicable.

Numerical work seems to have been pursued somewhat less although some simulations have been carried out by Dale & Sherwin (1996) for quasirealistic topography. However, in that work there was a vertical wall at the origin rather than a sloping beach, and the numerical procedure did not actually solve the eigenvalue problem, but instead adopted the *ad hoc* and pragmatic approach of looking for strong amplification in the response near certain frequencies.

The aim of this paper is to develop and implement a highly accurate numerical method to compute both the dispersion relation and the mode shapes for edge waves with rotation and stratification over general topography, and to complement this with an asymptotic analysis that refines, and sheds light on, previous approaches. The plan of the article is as follows: § 2 formulates the problem mathematically and reviews some semianalytic solutions; in § 3 the numerical scheme is developed; § 4 finds asymptotic solutions to the problem using classical WKBJ theory and a long-range uniform theory that corrects for certain deficiencies in the classical approach; their accuracy is cross-verified with the numerical scheme in § 5 and compared with other approximations from limiting cases; an investigation is made of trapped modes in the internal gravity wave (IGW) frequency band to demonstrate the utility of the methods developed; and some concluding remarks are provided in § 6.

2. Mathematical formulation and some analytic solutions

2.1. *Governing equations*

Our starting point is the set of equations presented by Llewellyn Smith (2004) – these are standard and well-known, see McKee (1973) – for the incompressible flow of an inviscid fluid over a gently sloping bottom, rotating with Coriolis frequency f. The x-axis points offshore, the y-axis along the shore, and the z-axis upwards. The undisturbed free surface of the fluid occupies the plane $z=0$. The bottom variation is assumed to depend only on the distance offshore and is defined by $z=-H(x)$, where $H(x)$ is monotonic increasing from $H(0)=0$. A pictorial representation is provided in figure 1. We adopt a base state of hydrostatic equilibrium, in which the base pressure $p_0(z)$ and base density $\rho_0(z)$ are related by $\mathrm{d}p_0/\mathrm{d}z = -\rho_0 g$, and we assume that disturbances are of sufficiently small amplitude to retain only linear terms in the equations formed by expanding about this state. Furthermore, we assume these disturbances are of the form $f(x,z)\exp[\mathrm{i}(\ell y-\omega t)]$, where $\omega>0$, without loss of

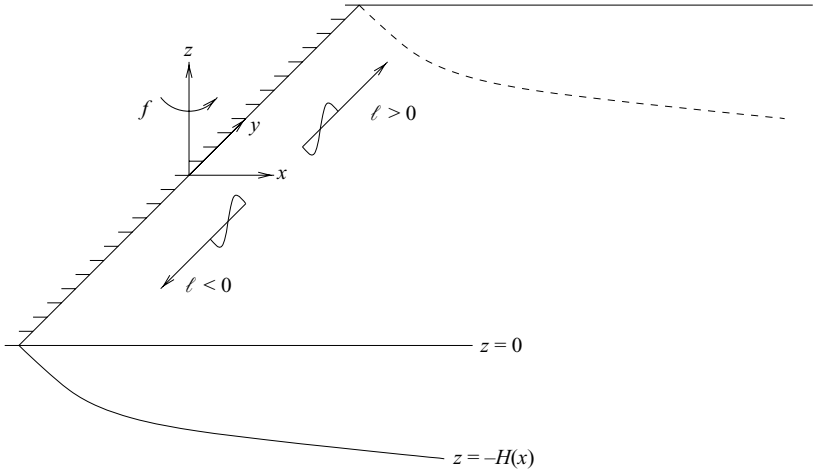

FIGURE 1. A pictorial representation of the physical problem. The directions of propagation for different signs of ℓ are also shown.

generality. Waves with $\ell > 0$ propagate with the shore on the left as shown in figure 1. The exponential factor is assumed understood and henceforth suppressed.

The resulting linearized equations can be expressed solely in terms of the perturbation pressure $p(x, z)$:

$$\nabla^2 p + \rho_0 \frac{\partial}{\partial z}\left[\frac{1}{\rho_0}\left(\frac{\omega^2 - f^2}{\omega^2 - N^2}\right)\frac{\partial p}{\partial z}\right] = 0, \quad -H(x) < z < 0, \tag{2.1}$$

$$\frac{\partial p}{\partial z} - \left(\frac{\omega^2 - N^2}{g}\right) p = 0, \quad z = 0, \tag{2.2}$$

$$\left(\frac{\omega^2 - f^2}{\omega^2 - N^2}\right)\frac{\partial p}{\partial z} + H'\frac{\partial p}{\partial x} - \frac{f\ell}{\omega}H' p = 0, \quad z = -H(x), \tag{2.3}$$

where the Laplacian is purely horizontal, the prime denotes differentiation and N is the Brunt–Väisälä (buoyancy) frequency defined by

$$N^2 = -\frac{g}{\rho_0}\frac{\mathrm{d}\rho_0}{\mathrm{d}z}. \tag{2.4}$$

We take this to be constant, corresponding to exponential density stratification, $\rho_0(z) = \mathrm{e}^{-bz}$, where $b = N^2/g$. Changing the dependent variable to $\phi = \mathrm{e}^{bz} p$ yields

$$s^2\phi_{zz} + \phi_{xx} - \left(\ell^2 + \frac{s^2 b^2}{4}\right)\phi = 0, \quad -H(x) < z < 0, \tag{2.5}$$

$$\phi_z - \lambda\phi = 0, \quad z = 0, \tag{2.6}$$

$$s^2\phi_z + H'\phi_x - \left(\frac{f\ell}{\omega}H' + \frac{s^2 b}{2}\right)\phi = 0, \quad z = -H(x), \tag{2.7}$$

where the subscripts denote partial differentiation with respect to those variables and

$$s^2 = \frac{\omega^2 - f^2}{\omega^2 - N^2}, \quad \lambda = \frac{\omega^2}{g} - \frac{b}{2}. \tag{2.8}$$

These are, to within a coordinate scaling, the equations of Llewellyn Smith. For trapped modes we also require that

$$\phi \to 0, \quad x \to \infty. \tag{2.9}$$

We shall make the oceanographically realistic assumption that, where these frequencies are non-zero, $0 < f < N$. The character of the governing partial differential equation changes from elliptic when s is real to hyperbolic when s is imaginary. The latter case corresponds to frequencies in the IGW band, $f < \omega < N$, within which the existence of trapped modes remains the subject of debate (Dale & Sherwin 1996; Pringle & Brink 1999; Llewellyn Smith 2004).

We briefly examine two solutions: the first is an analytic solution to the full governing equations for a bottom of constant slope; the second is a semianalytic solution inasmuch as it is an analytic solution to an approximate set of equations (those resulting from the shallow-water approximation) for a bottom tending exponentially to a constant depth offshore.

2.2. *Constant slope*

We specialize to a bottom of constant slope, $H(x) = \varepsilon x$, often referred to in the literature as a wedge. The existence of trapped edge waves for this idealized topography has been known since the work of Stokes (1846), who studied the problem without rotation and stratification. Ursell (1952) demonstrated that Stokes' solution was the lowest frequency member of a family of trapped modes, the size of the family depending on the slope ε. Evans (1989) provided a systematic method for constructing Ursell's modes based on the integral transform techniques of Whitham (1979) and used it to calculate the modes for the rotating problem. By scaling the vertical coordinate by s, Llewellyn Smith reduced (2.5)–(2.7) to the system considered by Evans and thus deduced the analytic solution for the rotating and stratified case. Using the auxiliary quantities

$$k^2 = \ell^2 + \frac{s^2 b^2}{4}, \ \beta = \tan^{-1}\left(\frac{\varepsilon}{s}\right), \ \alpha = -\left(\frac{f\ell}{\omega}\sin\beta + \frac{sb}{2}\cos\beta\right), \ \chi = \sin^{-1}\left(\frac{\alpha}{k}\right), \tag{2.10}$$

the wave function for the nth mode, up to an arbitrary multiplicative constant, can be written as

$$\begin{aligned}\phi_n(x,z) \ &= \mathrm{e}^{-k\left[x\cos(\beta-\chi)-s^{-1}z\sin(\beta-\chi)\right]} \\ &\quad + \sum_{m=1}^{n}\Big[A_{mn}\mathrm{e}^{-k\left\{x\cos[(2m-1)\beta-\chi]+s^{-1}z\sin[(2m-1)\beta-\chi]\right\}} \\ &\quad + \ B_{mn}\mathrm{e}^{-k\left\{x\cos[(2m+1)\beta-\chi]-s^{-1}z\sin[(2m+1)\beta-\chi]\right\}}\Big], \quad n = 0, 1, \ldots,\end{aligned} \tag{2.11}$$

where the sum is only taken for $n \geqslant 1$ and has coefficients

$$B_{mn} = (-1)^m \prod_{r=1}^{m} \frac{\tan[(n+1-r)\beta]\tan(r\beta-\chi)}{\tan(r\beta)\tan[(r+n)\beta-\chi]}, \quad A_{mn} = \frac{\tan(m\beta)}{\tan(m\beta-\chi)}B_{mn}. \tag{2.12}$$

The dispersion relation connecting ω and ℓ can be written

$$s\lambda + \alpha\cos[(2n+1)\beta] = (k^2-\alpha^2)^{1/2}\sin[(2n+1)\beta], \tag{2.13}$$

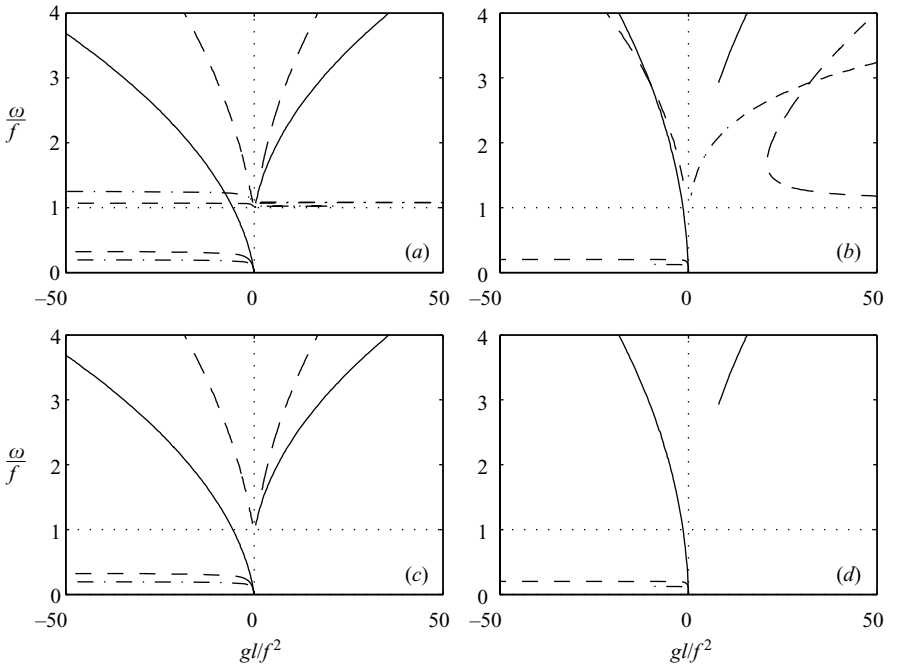

FIGURE 2. Dispersion curves for zeroth (solid line), first (dashed), and second (dot-dash) modes in a rotating wedge with no stratification; (*a*) 20° slope and (*b*) 70° slope, before discarding spurious roots; (*c*) 20° slope and (*d*) 70° slope, after discarding spurious roots.

subject to the decay condition (2.9) which requires that all x-exponents in (2.11) be negative:

$$k\cos(m\beta - \chi) > 0, \quad m = 1, \ldots, 2n+1. \tag{2.14}$$

For real s Evans required that

$$(2n+1)\beta - \chi < \frac{\pi}{2}, \tag{2.15}$$

so (2.14) is automatically satisfied for all n less than this upper bound. However, if Evans' solution is analytically continued to imaginary s (the IGW band), k and the argument of the cosine may be imaginary and so the full trapping condition (2.14) must be applied. Squaring both sides of (2.13) allows it to be recast as a quadratic equation for ℓ given ω. This quadratic has two branches, the first whose roots solve (2.13) and the second whose roots solve the same equation but with a negative right-hand side. We take this opportunity to correct a small oversight in Llewellyn Smith by noting that roots from this second branch must be discarded. Figure 2 shows figure 2 in Llewellyn Smith (dispersion curves for rotating, unstratified wedges of 20° and 70° slopes) before and after discarding these spurious roots, and similar corrections are required to figures 1 and 3 of that article.

2.3. *Exponential topography*

Ball (1967) applied the shallow-water approximation (see, e.g., Pedlosky 1987) to the case of a rotating bottom tending exponentially to a constant depth, often used as a simple model of a continental shelf or oceanic abyss:

$$H(x) = H_0\left(1 - \mathrm{e}^{-ax}\right). \tag{2.16}$$

We note that one of the assumptions of this approximation is that there is no density stratification, so this is necessarily excluded from Ball's work. Under this approximation the governing equations are reduced to a single ordinary differential equation which, after a suitable change of variable, yields a solution in terms of a confluent hypergeometric function. We shall confine our interest in Ball's solution to the alongshore wavenumber ℓ. Defining dimensionless quantities by

$$L = \frac{\ell}{a}, \quad \Omega^2 = \frac{\omega^2}{ga^2H_0}, \quad F^2 = \frac{f^2}{ga^2H_0}, \tag{2.17}$$

the wavenumbers are found to be the roots of

$$L^2 = \frac{FL}{\Omega} + (p+n)(p+n+1), \quad \text{where} \quad p^2 = L^2 + F^2 - \Omega^2, \tag{2.18}$$

and n, as before, is the mode number. The trapping condition is simply $p > 0$. The slope is characterized by its value at the shoreline, $\varepsilon = aH_0$. The shallow-water approximation requires $\varepsilon \ll 1$ and solutions of the equations derived under this approximation should resemble the solutions of the full equations with accuracy $O(\varepsilon^2)$.

3. Numerical method

In this section we describe the numerical method used to solve (2.5)–(2.7) and (2.9). It is assumed that f and N are given. The aim is to fix one of ω and ℓ and find the other, together with the corresponding wave function. Since ω is embedded rather awkwardly in s, it is convenient to fix ω and find ℓ. We note that ℓ appears quadratically in (2.5) and linearly in (2.7), so the system constitutes a nonlinear differential eigenvalue problem in which ℓ is the eigenvalue and ϕ the eigenfunction. Such nonlinear problems are typically difficult to solve, either numerically or analytically. Standard numerical techniques for linear problems, which involve recasting the problem in the form of a matrix eigenvalue equation, are no longer applicable. Instead an approach based on Newton–Kantorovich (NK) iteration is developed (see, e.g., Boyd 2001). For simplicity we shall illustrate the method by applying it to the constant slope of § 2.2, and then describe how it is adapted for general topographies.

The ith iterates of $\phi(x,z)$ and ℓ are denoted by $\phi^{(i)}(x,z)$ and $\ell^{(i)}$. Small quantities $\Delta(x,z)$ and δ are defined such that

$$\phi^{(i+1)} = \phi^{(i)} + \Delta, \quad \ell^{(i+1)} = \ell^{(i)} + \delta. \tag{3.1}$$

At each step the governing equations are assumed to hold exactly for $\phi^{(i+1)}$ and $\ell^{(i+1)}$. Substituting these into (2.5)–(2.7) and neglecting the $O(\delta\Delta)$ and $O(\delta^2)$ terms yields

$$\left[s^2\frac{\partial^2}{\partial z^2} + \frac{\partial^2}{\partial x^2} - \left(\ell^{(i)2} + \frac{s^2b^2}{4}\right)\right]\Delta - 2\ell^{(i)}\phi^{(i)}\delta = -\left[\ \ldots\ \right]\phi^{(i)}, \tag{3.2}$$

$$\left[\frac{\partial}{\partial z} - \lambda\right]\Delta = -\left[\ \ldots\ \right]\phi^{(i)}, \tag{3.3}$$

$$\left[s^2\frac{\partial}{\partial z} + H'\frac{\partial}{\partial x} - \left(\frac{f\ell^{(i)}}{\omega}H' + \frac{s^2b}{2}\right)\right]\Delta - \frac{f}{\omega}H'\phi^{(i)}\delta = -\left[\ \ldots\ \right]\phi^{(i)}, \tag{3.4}$$

where the shorthand $[\ldots]$ denotes the same bracketed differential operator as on the left-hand side. Since the governing equations are linear with respect to ϕ, ϕ is

only defined up to an arbitrary multiplicative constant. However, the iterative scheme requires a unique solution upon which to converge, so this constant must be specified. This is achieved by requiring that the value of ϕ at an arbitrary non-nodal point does not change from one iteration to the next:

$$\Delta(x_0, z_0) = 0, \quad \phi(x_0, z_0) \neq 0. \tag{3.5}$$

Spectral methods are used to solve (3.2)–(3.5). For the wedge, $H(x) = \varepsilon x$, the grid is constructed in plane polar coordinates in the sector $0 \leqslant r < \infty$, $-\arctan\varepsilon \leqslant \theta \leqslant 0$. The differential operators in (3.2)–(3.4) are found to contain terms in $1/r$ and $1/r^2$, which have removable singularities at the shoreline. These are eliminated by application of l'Hôpital's rule in the limit $r \to 0$. A p-point Laguerre scheme is used for the r-domain, thereby automatically incorporating the decay condition, and a q-point Chebyshev scheme is used for the θ-domain. The result is a matrix equation of the form

$$\boldsymbol{M}\boldsymbol{d} = \boldsymbol{u}, \tag{3.6}$$

where $\boldsymbol{M}$ is a $(pq+1) \times (pq+1)$ matrix and $\boldsymbol{d} = (\Delta(r_1, \theta_1), \ldots, \Delta(r_p, \theta_q), \delta)^T$. One of the grid points is chosen to be the point of constant ϕ in (3.5). The matrix equation is solved at each iteration by Gaussian elimination and the resulting values of Δ and δ are used to calculate the next iterates of ϕ and ℓ. The iteration loop terminates when $|\delta|$ becomes smaller than a specified tolerance.

The accuracy of this scheme is verified by comparison with the analytic solution of the previous section. The equations for non-zero f and N are solved using the analytic solution for $f = N = 0$ as the initial guess: typically the scheme required five iterations to find ℓ accurate to ten digits, and the wave function was similarly accurate. Considerable confidence may be placed in this scheme.

Finally, we turn to general topography. The problem here is that, in general, the domain $-H(x) < z < 0$ is not naturally suited to the grids used in spectral methods. Therefore, before constructing the NK scheme, it is necessary to transform the domain to something simpler (at the expense of making the governing equations more complicated). The most natural choice is to map the general bottom, $z = -H(x)$, to a wedge of equal initial slope, $z = -H'(0)x$, whilst leaving the free surface, $z = 0$, unchanged. This is achieved by the coordinate transformation:

$$u = x, \quad v = \mu(x)z, \quad \text{where} \quad \mu(x) = \frac{H'(0)x}{H(x)}. \tag{3.7}$$

The governing equations become:

$$\phi_{uu} + \frac{2\mu' v}{\mu}\phi_{uv} + \left[s^2\mu^2 + \left(\frac{\mu' v}{\mu}\right)^2\right]\phi_{vv} + \frac{\mu'' v}{\mu}\phi_v - \left(\ell^2 + \frac{s^2 b^2}{4}\right)\phi = 0, \tag{3.8}$$

$$\mu\phi_v - \lambda\phi = 0 \quad \text{on} \quad v = 0, \tag{3.9}$$

$$H'\phi_u + \left(s^2\mu + \frac{\mu' v}{\mu}H'\right)\phi_v - \left(\frac{f\ell}{\omega}H' + \frac{s^2 b}{2}\right)\phi = 0 \quad \text{on} \quad v = -H'(0)u. \tag{3.10}$$

The NK scheme is applied to these equations with a suitable initial guess. For slowly varying bottoms, which locally resemble constant slopes, it is usually possible to seed the iterative loop with the corresponding analytic solution for a wedge. Highly-deformed topographies or frequencies for which the desired mode does not exist in the wedge can be handled using a continuation method in which the scheme is run repeatedly as the topography or frequency is gradually changed from a known solution, the result for the previous choice being used to seed the loop for the next.

4. Asymptotic approaches

Asymptotic methods for trapped waves in oceanography were pioneered by Shen, Meyer & Keller (1968), who used a classical WKBJ approximation which is singular at shorelines and caustics. This analysis was refined by Shen & Keller (1975) using the idea of uniform approximations developed by Langer (1931), Kravtsov (1964) and Ludwig (1966). This approach involves replacing the exponential in the classical WKBJ approximation by a function with appropriate properties at shorelines and caustics such that the approximation is smooth there. This function is typically defined by a second-order ordinary differential equation known as the comparison equation.

As mentioned in § 2.2, an alternative approach employing the integral transform techniques of Whitham (1979) was used by Evans (1989) to incorporate rotation and stratification into the wedge problem. This was extended to gentle, arbitrary topographies by Zhevandrov (1991) and Sun & Shen (1994). Although these studies only deal explicitly with rotation, Llewellyn Smith (2004) deduced the corresponding results for stratification by rescaling variables. Zhevandrov also considered the uniform approximation, but with a different comparison equation from Shen & Keller. This naturally poses the question of which is superior and, indeed, why they are different at all.

Shen *et al.* and Shen & Keller used the classical form of ansatz in which only the amplitude, and not the phase, is expanded in powers of the small parameter. Smith (1977) pointed out a deficiency of this approach: it can lead to the asymptotic expansion becoming disordered for waves propagating over large distances. His remedy was to expand both amplitude and phase and to add an imaginary correction to the amplitude. The latter is equivalent to letting the phase depend on coordinates transverse to the direction of propagation, and this approach has been used in recent wave propagation and trapping studies in acoustics (see Adamou *et al.* 2005 and references therein). This form of expansion is also referred to in the literature as uniform: to avoid confusion with the concept of uniformity at shorelines and caustics, we shall refer to it as long-range. Although not strictly necessary for the problem at hand, since the waves do not propagate over long distances but are confined close to the shore, this refinement is not only potentially important in propagation problems, but also more intuitive in the sense that the resulting phase and amplitude functions actually correspond to the true phase and amplitude of the wave field.

The plan of this section is as follows: the classical WKBJ ansatz of Shen *et al.* (i.e., short-range and non-uniform) is applied to the problem with, for simplicity, $f = N = 0$. It is shown (in Appendix A) that the results for non-zero f and N, previously requiring the integral transform techniques of Whitham, can be obtained by this comparatively straightforward method. The two refinements are then applied to this method. We show that the long-range uniform approximation is, in some important respects, simpler and more intuitive than the classical WKBJ method. Finally, the differences arising from the choice of comparison equation are examined in detail.

4.1. *Classical WKBJ approximation*

We consider the non-rotating, non-stratified case ($s = 1$, $b = 0$, $\lambda = \omega^2/g$) and introduce a slow variable, $\xi = \varepsilon x$, where $\varepsilon \ll 1$. The governing equations (2.5)–(2.7) become

$$\phi_{zz} + \varepsilon^2 \phi_{\xi\xi} - \ell^2 \phi = 0, \qquad -h(\xi) < z < 0, \tag{4.1}$$

$$\phi_z - \lambda \phi = 0, \qquad z = 0, \tag{4.2}$$

$$\phi_z + \varepsilon^2 h' \phi_\xi = 0, \qquad z = -h(\xi), \tag{4.3}$$

where $h(\xi) = H(x)$.

We use the classical WKBJ ansatz,

$$\phi \sim \mathrm{e}^{S(\xi)/\varepsilon} \sum_{j=0}^{\infty} \varepsilon^j A^{(j)}(\xi, z), \tag{4.4}$$

in which only the amplitude is expanded in powers of ε. Substitution into (4.1)–(4.3) yields:

$$\sum_{j=0}^{\infty} \varepsilon^j \left[A^{(j)}{}_{zz} - (\ell^2 - S'^2) A^{(j)} + 2S' A^{(j-1)}{}_{\xi} + S'' A^{(j-1)} + A^{(j-2)}{}_{\xi\xi} \right] = 0, \tag{4.5}$$

$$\sum_{j=0}^{\infty} \varepsilon^j \left[A^{(j)}{}_{z} - \lambda A^{(j)} \right] = 0, \tag{4.6}$$

$$\sum_{j=0}^{\infty} \varepsilon^j \left[A^{(j)}{}_{z} + h' S' A^{(j-1)} + h' A^{(j-2)}{}_{\xi} \right] = 0. \tag{4.7}$$

We solve this hierarchy of equations from the lowest order up. The $j = 0$ equations are:

$$A^{(0)}{}_{zz} - (\ell^2 - S'^2) A^{(0)} = 0, \qquad 0 < z < -h(\xi), \tag{4.8}$$

$$A^{(0)}{}_{z} = \lambda A^{(0)}, \qquad z = 0, \tag{4.9}$$

$$A^{(0)}{}_{z} = 0, \qquad z = -h(\xi). \tag{4.10}$$

Defining $\kappa^2 = \ell^2 - S'^2$, the solution satisfying (4.8) and (4.10) is

$$A^{(0)} = f(\xi) \cosh\left[\kappa(z + h)\right]. \tag{4.11}$$

It will prove useful later to write this as $A^{(0)} = a_0(\xi)\psi(\xi, z)$, where

$$\psi = \left[\frac{h}{2} \left(1 + \frac{\sinh(2\kappa h)}{2\kappa h} \right) \right]^{-1/2} \cosh\left[\kappa(z + h)\right] \tag{4.12}$$

is normalized such that

$$\int_{-h}^{0} \psi^2 \, \mathrm{d}z = 1. \tag{4.13}$$

Satisfaction of (4.9) yields

$$\kappa \tanh(\kappa h) = \lambda, \tag{4.14}$$

which defines $\kappa(\xi)$ implicitly. We note that $\kappa = \ell$ at the caustic, $\xi = \xi_c$, hence

$$\ell \tanh[\ell h(\xi_c)] = \lambda. \tag{4.15}$$

For $h(\xi)$ monotonic increasing, we expect oscillatory solutions for $\xi < \xi_c$, where $S'^2 < 0$, and exponentially decaying solutions for $\xi > \xi_c$, where $S'^2 > 0$.

We proceed to the $j = 1$ equations to determine $a_0(\xi)$:

$$A^{(1)}{}_{zz} - \kappa^2 A^{(1)} = -(S' A^{(0)2})_{\xi} / A^{(0)}, \qquad 0 < z < -h(\xi), \tag{4.16}$$

$$A^{(1)}{}_{z} = \lambda A^{(1)}, \qquad z = 0, \tag{4.17}$$

$$A^{(1)}{}_{z} = -h' S' A^{(0)}, \qquad z = -h(\xi). \tag{4.18}$$

The transport equation for a_0 is extracted by multiplying (4.16) by $A^{(0)}$ and integrating over the depth. After integrating by parts twice, the left-hand side is

$$\left[A^{(0)}A^{(1)}{}_z - A^{(0)}{}_z A^{(1)}\right]_{-h}^{0} + \int_{-h}^{0} A^{(1)}\left(\frac{\partial^2}{\partial z^2} - \kappa^2\right) A^{(0)}\,\mathrm{d}z. \tag{4.19}$$

The integrand is zero by (4.8) and the boundary term can be simplified using the boundary conditions on $A^{(0)}$ and $A^{(1)}$ to give $h'S'A^{(0)^2}(\xi, -h)$. Turning our attention to the right-hand side, we get

$$\begin{aligned}\text{right-hand side} &= -\int_{-h}^{0} \frac{\partial}{\partial \xi}\left(S'A^{(0)^2}\right)\mathrm{d}z \\ &= -\frac{\mathrm{d}}{\mathrm{d}\xi}\int_{-h}^{0} S'A^{(0)^2}\,\mathrm{d}z + h'S'A^{(0)^2}(\xi, -h) \\ &= -\frac{\mathrm{d}}{\mathrm{d}\xi}\left(S'a_0^2\int_{-h}^{0}\psi^2\,\mathrm{d}z\right) + h'S'A^{(0)^2}(\xi, -h) \\ &= -\left(S'a_0^2\right)' + h'S'A^{(0)^2}(\xi, -h),\end{aligned} \tag{4.20}$$

since the integral in the third line is unity by (4.13). The second term cancels with the left-hand side to give the transport equation,

$$\left(S'a_0^2\right)' = 0, \tag{4.21}$$

from which we obtain, up to an arbitrary multiplicative constant, $a_0(\xi) = S'^{-1/2}$.

We are now in a position to construct the solution. The solution decaying in $\xi > \xi_c$ is

$$\begin{aligned}\phi &= \psi(\xi, z)[S'(\xi)]^{-1/2}\exp\left[-\frac{1}{\varepsilon}\int_{\xi_c}^{\xi} S'(\xi)\,\mathrm{d}\xi\right] \\ &= \psi(\xi, z)\left[\ell^2 - \kappa^2(\xi)\right]^{-1/4}\exp\left\{-\frac{1}{\varepsilon}\int_{\xi_c}^{\xi}\left[\ell^2 - \kappa^2(\xi)\right]^{1/2}\mathrm{d}\xi\right\}.\end{aligned} \tag{4.22}$$

For $\xi < \xi_c$, the WKBJ connection formula gives (see e.g. Bender & Orszag 1978, Eq. 10.4.13c)

$$\phi = 2\psi(\xi, z)[\kappa^2(\xi) - \ell^2]^{-1/4}\sin\left\{\frac{1}{\varepsilon}\int_{\xi}^{\xi_c}[\kappa^2(\xi) - \ell^2]^{1/2}\mathrm{d}\xi + \frac{\pi}{4}\right\}. \tag{4.23}$$

We note that both expressions are singular at the caustic. This is a feature of the classical WKBJ approximation. They are also singular at the shoreline since ψ contains the factor $h^{-1/2}$. Finally, we have the constraint

$$\frac{1}{\varepsilon}\int_{0}^{\xi_c}\left[\kappa^2(\xi) - \ell^2\right]^{1/2}\mathrm{d}\xi \sim \left(n + \frac{1}{2}\right)\pi + O(\varepsilon), \quad n = 0, 1, \ldots, \tag{4.24}$$

which connects ω and ℓ for a given mode number n. This asymptotic dispersion relation was first derived rigorously by Shen *et al.* but can be viewed heuristically as an extension of the two-turning-point constraint of Bender & Orszag (1978, Eq. 10.5.2) in which the shoreline, $\xi = 0$, is the second turning point. The integral approaches its maximum value as $\xi_c \to \infty$, so there is an upper bound on n:

$$n \leqslant \frac{1}{\pi\varepsilon}\lim_{\xi_c\to\infty}\left\{\int_{0}^{\xi_c}[\kappa^2(\xi) - \ell^2]^{1/2}\mathrm{d}\xi\right\} - \frac{1}{2}. \tag{4.25}$$

This upper bound varies with the bottom profile, h, so modes may not be stable with respect to changes in the profile.

4.1.1. *Example: wedge*

For the wedge, $h(\xi)=\xi$, the integral in (4.24) can be evaluated in closed form. It is $(\pi/2)\arcsin(\lambda/\ell)$ and so the dispersion relation is

$$\lambda \sim \ell \sin[(2n+1)\varepsilon]. \tag{4.26}$$

Ursell's (1952) exact dispersion relation is

$$\lambda = \ell \sin[(2n+1)\arctan\varepsilon], \tag{4.27}$$

so (4.26) is accurate to $O(\varepsilon^2)$ provided $n \ll 1/\varepsilon$. Condition (4.25) is now

$$n \leqslant \frac{1}{\pi\varepsilon} \lim_{\xi_c\to\infty} \left[\frac{\pi}{2}\arcsin\left(\frac{\lambda}{\ell}\right)\right] - \frac{1}{2}, \tag{4.28}$$

and, since $\lambda/\ell \to 1$ as $\xi_c \to \infty$ from (4.15), the upper bound on n is

$$n \leqslant \frac{\pi}{4\varepsilon} - \frac{1}{2}, \tag{4.29}$$

which also agrees with Ursell.

4.2. *Long-range uniform approximation*

The classical WKBJ approximation to the wave function is singular at the shoreline and caustic and is therefore inaccurate in the neighbourhoods of these points. This deficiency is overcome by a refinement of the classical method known as the uniform approximation. This is constructed by replacing the exponential with a function, V, that behaves appropriately in the vicinities of the shoreline and caustic and exponentially elsewhere. To avoid confusion with the previous calculation we denote by ρ the phase-like function. V is defined as the solution of a second-order ordinary differential equation known as the comparison equation,

$$V''(\rho/\varepsilon) + \varepsilon P(\rho)V'(\rho/\varepsilon) + Q^2(\rho)V(\rho/\varepsilon) = 0, \tag{4.30}$$

which is regular at the shoreline and caustic and decays as $\rho \to \infty$. The caustic corresponds to $Q=0$. Away from singularities of P and zeros of Q, the comparison equation reduces in the limit $\varepsilon \to 0$ to

$$V'' + (\text{constant})V = 0, \tag{4.31}$$

which gives exponential behaviour appropriate for regions away from the shoreline and caustic, whose positions are therefore given by these singularities and/or zeros. Without loss of generality we let $\rho=0$ at the shoreline and denote the caustic by $\rho=\rho_c$. The theory developed by Langer, Kravtsov, Ludwig and others states that, in a small neighbourhood of the shoreline, the comparison equation must reduce to the zeroth-order Bessel equation and, in a small neighbourhood of the caustic, to the Airy equation as $\varepsilon \to 0$. By choosing P and Q appropriately it is possible to construct systematically a comparison equation for any combination of shorelines and caustics. The comparison equation is not unique: Shen & Keller use

$$P = \frac{1}{\rho}, \quad Q = (\rho_c - \rho)^{1/2}, \tag{4.32}$$

whereas Zhevandrov uses

$$P = \frac{1}{\rho}, \quad Q = \left(\frac{\rho_c - \rho}{\rho}\right)^{1/2}. \tag{4.33}$$

Provided it satisfies the above conditions, the choice of comparison equation is in some sense immaterial, in that the approximations to the wave functions that result from two different choices of V will simply have different phase functions $\rho(\xi, z)$ such that they are asymptotically identical. However, it will be shown that the choice does have a subtle effect on the leading-order dispersion relation.

Our starting point is the ansatz

$$\phi(\xi, z) = A(\xi, z) V[\varepsilon^{-1}\rho(\xi, z)], \tag{4.34}$$

where both A and ρ are to be expanded in powers of ε:

$$A(\xi, z) \sim \sum_{j=0}^{\infty} \varepsilon^j A^{(j)}(\xi, z), \qquad \rho(\xi, z) \sim \sum_{j=0}^{\infty} \varepsilon^j \rho^{(j)}(\xi, z). \tag{4.35}$$

Differentiating ϕ with respect to ξ and making use of the comparison equation to express V'' in terms of V and V' gives

$$\phi_\xi = A_\xi V + \varepsilon^{-1}\rho_\xi A V', \tag{4.36}$$

$$\phi_{\xi\xi} = \left(A_{\xi\xi} - \varepsilon^{-2}\rho_\xi^2 Q^2 A\right) V + \varepsilon^{-1}\left(2\rho_\xi A_\xi + \rho_{\xi\xi} A - \rho_\xi^2 P A\right) V', \tag{4.37}$$

and similarly for z. Substitution into (4.1)–(4.3) yields

$$\left[-\varepsilon^{-2}\rho_z^2 Q^2 A + A_{zz} - \left(\ell^2 + \rho_\xi^2 Q^2\right) A + \varepsilon^2 A_{\xi\xi}\right] V + \left\{\varepsilon^{-1}\left[(\rho_z A^2)_z / A - \rho_z^2 P A\right] + \varepsilon\left[(\rho_\xi A^2)_\xi / A - \rho_\xi^2 P A\right]\right\} V' = 0, \tag{4.38}$$

$$(A_z - \lambda A) V + \varepsilon^{-1}\rho_z A V' = 0, \tag{4.39}$$

$$(A_z + \varepsilon^2 h' A_\xi) V + (\varepsilon^{-1}\rho_z A + \varepsilon h' \rho_\xi A) V' = 0. \tag{4.40}$$

The expansions for A and ρ are inserted to form a hierarchy of equations in powers of ε. Taylor's theorem is used to expand $P(\rho)$ and $Q(\rho)$ about $\rho^{(0)}$.

At $O(\varepsilon^{-2})$ we find immediately that ${\rho^{(0)}}_z = 0$, whence the $O(\varepsilon^{-1})$ equations are trivially satisfied. At $O(1)$ the coefficients of V and V' are equated to zero separately to give two governing equations and four boundary conditions:

$$A^{(0)}_{zz} - \left[\ell^2 + \left({\rho^{(0)}_\xi}^2 + {\rho^{(1)}_z}^2\right) Q^2(\rho^{(0)})\right] A^{(0)} = 0, \qquad 0 < z < -h(\xi), \tag{4.41}$$

$$\left(\rho^{(1)}{}_z A^{(0)2}\right)_z / A^{(0)} = 0, \qquad 0 < z < -h(\xi), \tag{4.42}$$

$$A^{(0)}{}_z = \lambda A^{(0)}, \quad \rho^{(1)}{}_z A^{(0)} = 0, \qquad z = 0, \tag{4.43}$$

$$A^{(0)}{}_z = 0, \quad \rho^{(1)}{}_z A^{(0)} = 0, \qquad z = -h(\xi). \tag{4.44}$$

Together (4.42) and (4.43*b*) imply that, since $A^{(0)} \neq 0$, we must have ${\rho^{(1)}}_z = 0$. Then (4.41) becomes

$$A^{(0)}_{zz} - \left\{\ell^2 + [\rho^{(0)}_\xi Q(\rho^{(0)})]^2\right\} A^{(0)} = 0. \tag{4.45}$$

Thus, (4.43*a*) and (4.44*a*) are identical to the corresponding equations in the classical approximation, (4.8)–(4.10), except that $-S'^2$ has been replaced by $[\rho^{(0)}_\xi Q(\rho^{(0)})]^2$. Redefining $\kappa^2 = \ell^2 + [\rho^{(0)}_\xi Q(\rho^{(0)})]^2$, the solutions can be written

$$A^{(0)} = a_0(\xi)\psi(\xi, z), \tag{4.46}$$

where ψ is as defined in (4.12) and κ is given implicitly by (4.14). The definition of κ gives the leading-order phase $\rho^{(0)}(\xi)$ by

$$\int_{\rho^{(0)}}^{\rho_c} Q(\rho)\,\mathrm{d}\rho = \int_{\xi}^{\xi_c} [\kappa^2(\xi) - \ell^2]^{1/2}\,\mathrm{d}\xi, \qquad 0 < \xi < \xi_c, \tag{4.47}$$

$$\int_{\rho_c}^{\rho^{(0)}} [-Q^2(\rho)]^{1/2}\,\mathrm{d}\rho = \int_{\xi_c}^{\xi} [\ell^2 - \kappa^2(\xi)]^{1/2}\,\mathrm{d}\xi, \qquad \xi > \xi_c. \tag{4.48}$$

The $O(\varepsilon)$ equations are

$$A^{(1)}{}_{zz} - \kappa^2 A^{(1)} = 2\rho^{(0)}{}_{\xi} Q(\rho^{(0)}) \left[\rho^{(1)} Q(\rho^{(0)})\right]_{\xi} A^{(0)}, \quad 0 < z < -h(\xi), \tag{4.49}$$

$$\left(\rho^{(0)}{}_{\xi} A^{(0)2}\right)_{\xi} / A^{(0)} + \left(\rho^{(2)}{}_{z} A^{(0)2}\right)_{z} / A^{(0)} - \rho^{(0)}{}_{\xi}^{2} P(\rho^{(0)}) A^{(0)} = 0, \quad 0 < z < -h(\xi), \tag{4.50}$$

$$A^{(1)}{}_{z} = \lambda A^{(1)}, \quad \rho^{(2)}{}_{z} A^{(0)} = 0, \quad z = 0, \tag{4.51}$$

$$A^{(1)}{}_{z} = 0, \quad \rho^{(2)}{}_{z} A^{(0)} = -h'\rho^{(0)}{}_{\xi} A^{(0)}, \quad z = -h(\xi). \tag{4.52}$$

Following the calculation in (4.20), we multiply (4.50) by $A^{(0)}$, integrate over the depth, and apply the boundary conditions to get the transport equation for a_0,

$$(\rho^{(0)}{}_{\xi} a_0^2)_{\xi} - P(\rho^{(0)}) \rho^{(0)}{}_{\xi}^{2} a_0^2 = 0, \tag{4.53}$$

whose solution, up to an arbitrary multiplicative constant, can be written

$$a_0(\xi) = R(\rho^{(0)}) \left[\rho^{(0)}{}_{\xi} Q(\rho^{(0)})\right]^{-1/2} = R(\rho^{(0)}) [\kappa^2 - \ell^2]^{-1/4}, \tag{4.54}$$

where

$$R(\rho^{(0)}) = Q(\rho^{(0)})^{1/2} \exp\left[\frac{1}{2} \int^{\rho^{(0)}} P(\rho)\,\mathrm{d}\rho\right]. \tag{4.55}$$

The quantity $[\kappa^2 - \ell^2]^{-1/4}$ in (4.54) is simply the value of a_0 obtained in the classical theory. Therefore the function R, whose form is determined entirely by P and Q, tells us how the uniform theory modifies a_0 to remove the singularities in the leading-order amplitude at the shoreline and caustic. Shen & Keller's comparison equation leads to

$$R(\rho^{(0)}) = (\rho^{(0)} - \rho_c)^{1/4} \rho^{(0)\,1/2}, \tag{4.56}$$

whilst Zhevandrov's leads to

$$R(\rho^{(0)}) = (\rho^{(0)} - \rho_c)^{1/4} \rho^{(0)\,1/4}. \tag{4.57}$$

Both functions have zeros at the shoreline and caustic of the forms required to cancel the singularities in the classical amplitude. Returning to (4.49), we note that the boundary conditions (4.51*a*) and (4.52*a*) on $A^{(1)}$ are the same as those on $A^{(0)}$ in (4.41). Therefore, denoting by $A^{(1)}{}_{hom} = a_1(x)\psi(x, z)$ the solution to the homogeneous part, a solvability condition for (4.49) is obtained by integrating its product with $A^{(1)}{}_{hom}$ over the depth. As before, the left-hand side is zero, leaving

$$\begin{aligned} 0 &= 2\rho^{(0)}{}_{\xi} Q(\rho^{(0)}) [\rho^{(1)} Q(\rho^{(0)})]_{\xi} \int_{-h}^{0} A^{(0)} A^{(1)}{}_{hom}\,\mathrm{d}z \\ &= 2\rho^{(0)}{}_{\xi} Q(\rho^{(0)}) [\rho^{(1)} Q(\rho^{(0)})]_{\xi} a_0(\xi) a_1(\xi). \end{aligned} \tag{4.58}$$

For this to be true for all ξ requires

$$\rho^{(1)}(\xi) Q[\rho^{(0)}(\xi)] = \text{constant}. \tag{4.59}$$

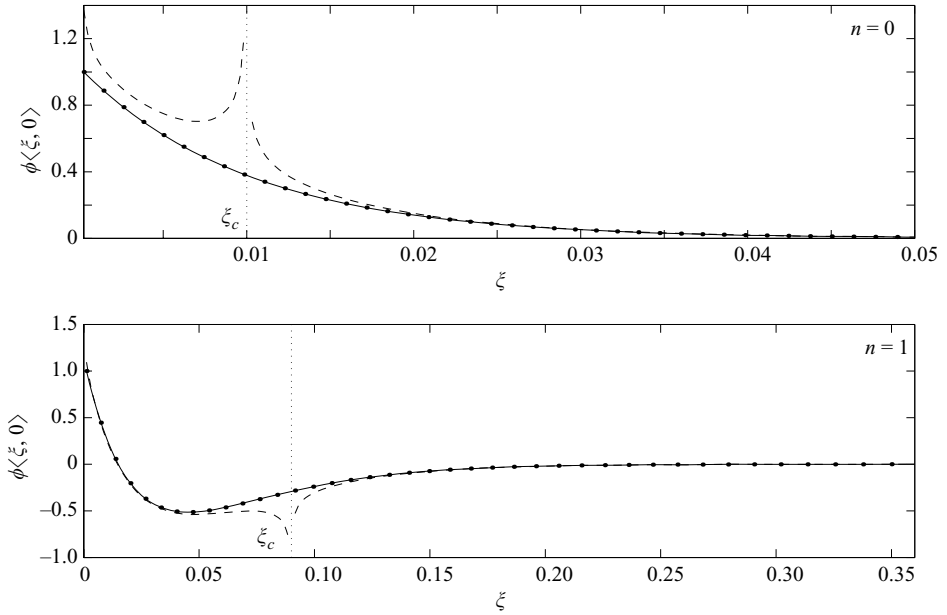

FIGURE 3. Uniform (solid line), WKBJ (dashed) and exact (dots) wave functions for the lowest two modes in a wedge of slope $\varepsilon = 0.1$ with no rotation or stratification for $\lambda = 1$. The caustic $\xi = \xi_c$ is shown by the vertical dotted line.

Evaluating this at the caustic, where $Q[\rho^{(0)}(\xi_c)] = 0$, and noting that $\rho^{(1)}$ cannot be singular since it is assumed to be an $O(1)$ quantity in the asymptotic expansion of ρ, we find that this constant is zero and hence $\rho^{(1)} = 0$.

Figure 3 shows the uniform approximation to the wave function in a wedge using Zhevandrov's comparison equation (Shen & Keller's wave function is indistinguishable from Zhevandrov's on this scale). Also shown are the classical WKBJ approximation, with its singularities at the shoreline and caustic, and the exact solution, to which the uniform wave function is seen to be an excellent approximation. Note also that the classical approximation is particularly poor in $\xi < \xi_c$ for the lowest mode. This is because the exact solution does not exhibit significant oscillatory behaviour in this region, but classical WKBJ theory imposes an oscillating function there.

All that remains is to find the asymptotic dispersion relation between ω and ℓ for a given mode n. Rather than appealing heuristically to the two-turning-point constraint of classical WKBJ theory, the uniform approximation allows the integral constraint to be put on a more concrete footing. Setting $\xi = 0$ in (4.47) and dividing by ε gives

$$\frac{1}{\varepsilon}\int_0^{\xi_c} \left[\kappa^2(\xi) - \ell^2\right]^{1/2} \mathrm{d}\xi = \frac{1}{\varepsilon}\int_0^{\rho_c} Q(\rho)\,\mathrm{d}\rho, \tag{4.60}$$

the left-hand side of which is the same as that of (4.24). The right-hand side depends on ρ_c, which has thus far remained unevaluated. We note that ρ_c always appears in the comparison equation in Q, which must be zero there, and may also appear in P. The requirements that V be regular at the shoreline and caustic and decay as $\rho \to \infty$ make the comparison equation, in effect, an eigenvalue problem with eigenvalues ${\rho_c}^{(n)}$ for $n \geqslant 0$. In general these must be extracted numerically, whereupon the right-hand side of (4.60) can be evaluated to give the asymptotic dispersion relation. Different

choices of comparison equation will produce different eigenvalues, giving rise to the question of what effect, if any, this has on the dispersion relation.

4.2.1. *Zhevandrov's comparison equation*

The eigenvalues of Zhevandrov's comparison equation, given by (4.33), are obtained analytically in Appendix B as $\rho_c^{(n)} = (2n+1)\varepsilon$ exactly. The right-hand side of (4.60) is

$$\frac{1}{\varepsilon}\int_0^{\rho_c}\left(\frac{\rho_c-\rho}{\rho}\right)^{1/2}\mathrm{d}\rho = \frac{1}{\varepsilon}\left[\sqrt{\rho(\rho_c-\rho)} - \rho_c \arctan\sqrt{\frac{\rho_c-\rho}{\rho}}\,\right]_0^{\rho_c} = \frac{\pi\rho_c}{2\varepsilon}. \tag{4.61}$$

Hence the asymptotic dispersion relation is

$$\frac{1}{\varepsilon}\int_0^{\xi_c}\left[\kappa^2(\xi)-\ell^2\right]^{1/2}\mathrm{d}\xi = \left(n+\frac{1}{2}\right)\pi, \quad n=0,1,\ldots, \tag{4.62}$$

which is, to leading order, the same as (4.24). This is a remarkable result: using a superior wave-function approximation, uniform at the shoreline and caustic, offers no improvement whatsoever to the leading-order approximation to the dispersion relation obtained using the classical WKBJ approximation, which is singular at these points. It indicates, usefully, that practitioners interested in only the spectra of problems like this can retreat to the less intensive calculations of classical theory with no loss of accuracy.

4.2.2. *Shen & Keller's comparison equation*

Setting $\rho = \varepsilon^{2/3}\zeta$ allows Shen & Keller's comparison equation, given by (4.32), to be written in a form whose eigenvalues are independent of ε:

$$\zeta V_{\zeta\zeta} + V_\zeta + \zeta(\zeta_c - \zeta)V = 0. \tag{4.63}$$

V is regular at $\zeta = 0, \zeta_c$ and decays as $\zeta \to \infty$. The eigenvalues $\zeta_c^{(n)}$ are obtained numerically using a Laguerre spectral method to impose the decay condition. The right-hand side of (4.60) is straightforward to evaluate:

$$\frac{1}{\varepsilon}\int_0^{\rho_c}(\rho_c-\rho)^{1/2}\mathrm{d}\rho = -\frac{1}{\varepsilon}\left[\frac{2}{3}(\rho_c-\rho)^{3/2}\right]_0^{\rho_c} = \frac{2{\rho_c}^{3/2}}{3\varepsilon}, \tag{4.64}$$

whence the asymptotic dispersion relation is

$$\frac{1}{\varepsilon}\int_0^{\xi_c}\left[\kappa^2(\xi)-\ell^2\right]^{1/2}\mathrm{d}\xi = \frac{2}{3}(\zeta_c^{(n)})^{3/2}, \quad n=0,1,\ldots. \tag{4.65}$$

The eigenvalues of (4.63) obtained numerically are found to be such that the right-hand side is close to $(n+1/2)\pi$. We write

$$\frac{2}{3}(\zeta_c^{(n)})^{3/2} = \left(n+\frac{1}{2}-\frac{\delta_n}{2}\right)\pi, \quad \delta_n \ll 1, \tag{4.66}$$

and tabulate the first five values of $\zeta_c^{(n)}$ and δ_n in table 1.

4.2.3. *Comparison for wedge*

Since the two comparison equations give slightly different dispersion relations, and Zhevandrov's appears to offer no improvement over classical WKBJ theory, it is interesting to compare them in more detail. Recall Ursell's exact dispersion relation for the wedge (4.27):

$$\lambda/\ell = \sin[(2n+1)\arctan\varepsilon]. \tag{4.67}$$

n	$\zeta_c^{(n)}$	δ_n
0	1.73722	2.8×10^{-2}
1	3.67023	1.6×10^{-2}
2	5.16974	1.1×10^{-2}
3	6.47400	8.7×10^{-3}
4	7.65712	7.4×10^{-3}

TABLE 1. The first five values of $\zeta_c^{(n)}$ and δ_n.

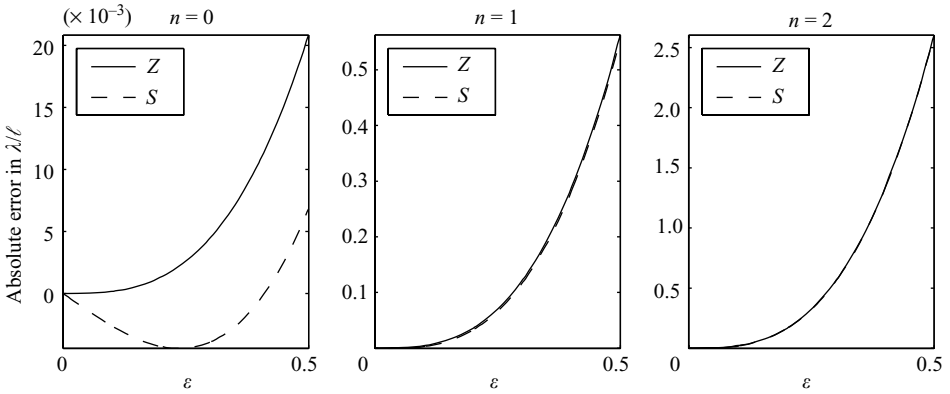

FIGURE 4. Absolute errors in λ/ℓ for the lowest three modes for Zhevandrov's (labelled Z) and Shen & Keller's (S) comparison equations.

Zhevandrov's comparison equation gives

$$\lambda/\ell = \sin[(2n+1)\varepsilon], \tag{4.68}$$

while Shen & Keller's comparison equation leads to

$$\lambda/\ell = \sin[(2n+1-\delta_n)\varepsilon]. \tag{4.69}$$

Taylor expanding in ε gives the absolute errors in these approximations to λ/ℓ as:

$$E_{Zhev} \sim \frac{(2n+1)\varepsilon^3}{3} + O(\varepsilon^5); \tag{4.70}$$

$$E_{Shen} \sim -\delta_n\varepsilon + \frac{(2n+1)\varepsilon^3}{3} + \frac{[(2n+1)^3 - (2n+1-\delta_n)^3]\varepsilon^3}{6} + O(\varepsilon^5). \tag{4.71}$$

Figure 4 compares the absolute errors for the lowest three modes for $0 \leqslant \varepsilon \leqslant 1/2$. For the lowest mode Zhevandrov's comparison equation provides the formally superior approximation in that the error converges monotonically to zero as $\varepsilon \to 0$. Shen & Keller's does not, but there is a range of ε for which the additional δ_n-dependent term in (4.71) cancels out the main term to give a smaller error: this range includes some physically realistic values of ε. For higher modes the factor $(2n+1)$ causes the main term to dominate so that the two approximations are hard to distinguish.

5. Results and discussion

The number of variables in this problem is large: varying the mode number n, the frequency ω, the physical parameters f, N and g and the bottom profile, including

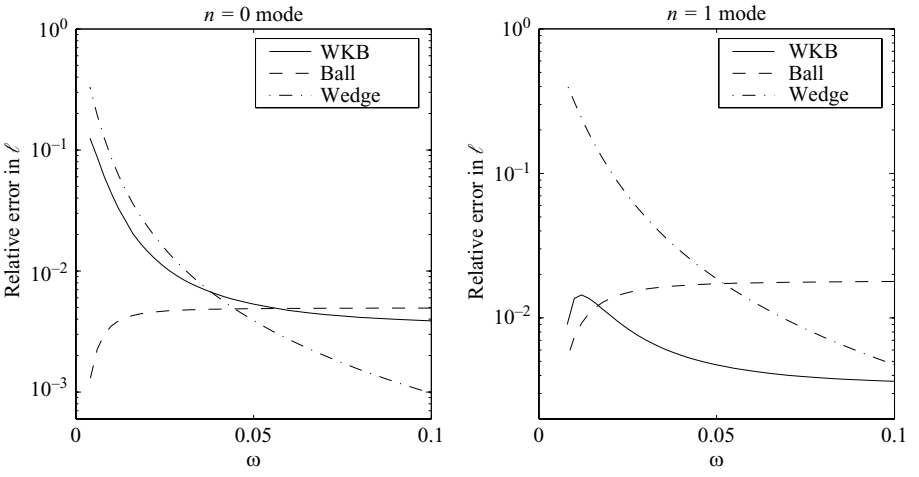

FIGURE 5. Relative errors in the values of ℓ obtained by WKBJ theory, by Ball's shallow-water approximation and by treating the topography as a wedge of slope ε for the lowest two modes of the $f = N = 0$ problem.

the slope scale ε, the depth scale h_∞ and the precise form of $h(\xi)$, will all produce different effects on the wavenumber ℓ and wave function ϕ. An investigation of the full parameter space would be an enormous undertaking, well outside the scope of this work. Instead, we begin this section by using the numerical scheme developed in § 3 to verify the accuracy of the asymptotic results of § 4 for Ball's (1967) exponential topography, and compare these to his shallow-water approximation and the crude approximation of treating the topography as a wedge. We then demonstrate the numerical scheme's power as an investigative tool by tracking a trapped mode in ω-space to determine two things: whether such modes can exist in the IGW frequency band ($f < \omega < N$), which is an open question (Dale & Sherwin 1996; Pringle & Brink 1999; Llewellyn Smith 2004); and at what frequency and for what physical reasons the mode ceases to be trapped. It was found that realistic oceanographic parameters did not produce suitable modes for this part of the study, so the parameters were hand-picked to expose the relevant physical phenomena as clearly as possible: these parameters could be reproduced in the laboratory. Finally, we conclude with a note on the oceanographic relevance of these results.

5.1. *Accuracy*

We use Ball's exponential topography (2.16) with $H_0 = 5 \times 10^3$ and $a = 2 \times 10^{-5}$ to give an initial slope of $\varepsilon = 0.1$ (5.7° angle) and take $g = 10$ (all in arbitrary units). In SI units this would be a reasonable model of an oceanic abyss minus the detail of the continental shelf. The classical WKBJ approximation to the wavenumber, which was shown in § 4.2 to be the same as the uniform approximation, is calculated from the relevant asymptotic dispersion relation, (4.24) for $f = N = 0$ or (A 17) (see Appendix A) otherwise, using Gaussian quadrature to evaluate the integral and an adaptive root-finding algorithm to locate ℓ. Ball's shallow-water approximation and the exact wavenumber for a wedge of slope ε (the same as the initial slope of the exponential topography) are obtained directly from expressions (2.18) and (2.13) respectively.

Figure 5 compares the relative errors between these three values of ℓ and the value calculated using the numerical scheme of § 3 for the lowest two modes of the

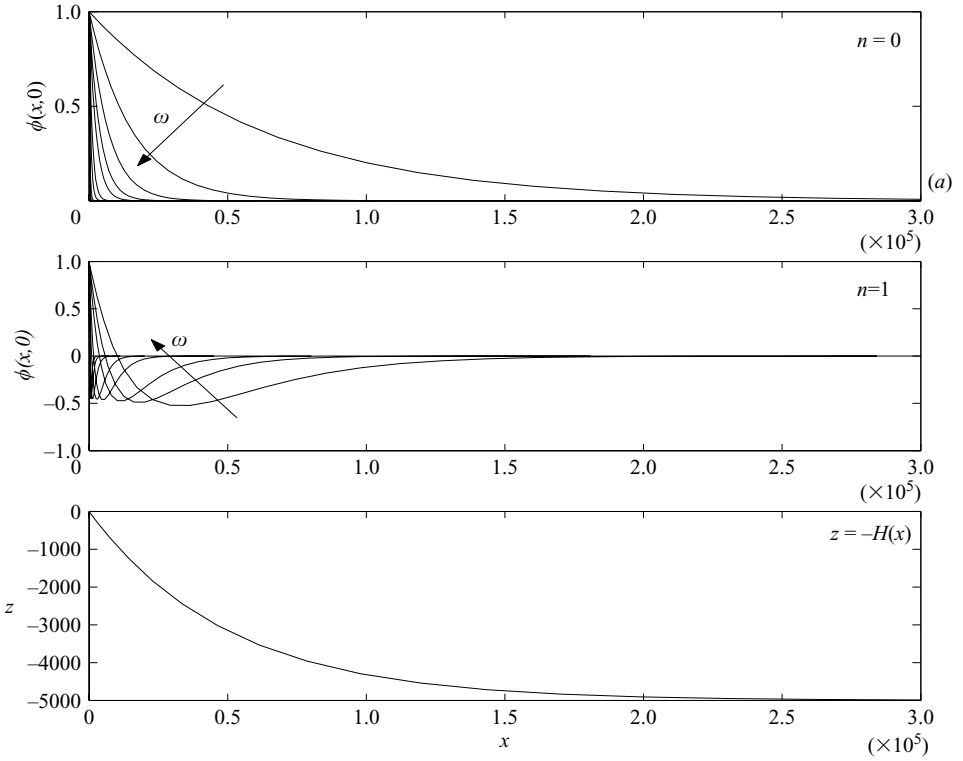

FIGURE 6. (a, b) The surface wave function for the lowest two modes as ω increases. (c) The bottom profile for reference. All three plots use the same horizontal scale.

$f = N = 0$ problem. The absence of rotation means there is no need to specify whether these modes are for $\ell > 0$ or $\ell < 0$ since these are just identical modes propagating in opposite directions. A notable feature of figure 5 is that, as ω increases, the value of ℓ obtained by treating the topography as a wedge becomes increasingly accurate. Indeed, for the lowest mode, it is superior to the other two approximations, which use the true topography. The reason for this is found in figure 6, which shows the wave becoming confined to an increasingly small region close to the shore as ω increases. This region eventually becomes so small that the bottom locally resembles a constant slope and the wave becomes virtually indistinguishable from that of a wedge.

The WKBJ approximation is less accurate for the $n = 0$ mode than for the $n = 1$ mode. The reason for this was established in figure 3 and the associated discussion. Nevertheless, the accuracy is around $O(\varepsilon^2)$ for most frequencies in the range shown, which is within the $O(\varepsilon)$ accuracy predicted by the asymptotic dispersion relation (4.24).

Ball's shallow-water approximation is accurate to $O(\varepsilon^2)$ as anticipated and does not vary much with ω. It becomes increasingly accurate as the wave moves further out to sea, filling more of the topography's exponential tail as it does so. There appears to be a slight decrease in accuracy as n increases: this is consistent with Ball's statement that the shallow-water approximation breaks down as $n \to 1/\varepsilon$.

Rotation is now added (but not stratification, since Ball's approximation would not apply). Figure 7 shows the relative errors in the WKBJ, Ball and wedge wavenumbers for the lowest two modes with $\ell > 0$ (coast on left) and $f = 0.01$. In SI units this would

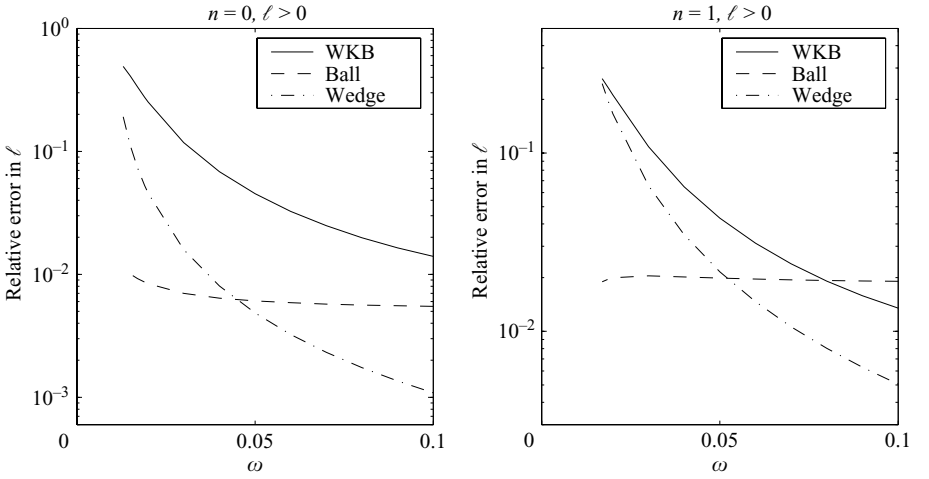

FIGURE 7. Relative errors in the values of ℓ obtained by WKBJ theory, by Ball's shallow-water approximation and by treating the topography as a wedge of slope ε for the lowest two $\ell > 0$ modes for $f = 0.01$ and no stratification.

be 2–3 orders of magnitude larger than a realistic oceanographic value (depending on latitude). The Ball and wedge wavenumbers are found to be as described for the non-rotating case. The WKBJ approximation performs somewhat less well but, for most frequencies in the range, remains within its predicted accuracy.

5.2. *Internal gravity waves*

We use the parameters above except that a is adjusted to give an initial angle of 20° and stratification is introduced by setting $N = 3f$. As noted above, these parameters are not oceanographically realistic. They have been hand-picked for the purposes of this investigation into IGWs but could be reproduced in the laboratory.

Figure 8(*a*) shows the dispersion curves, calculated from the analytical solution, for the lowest three modes in a 20° wedge with $N = 3f$. This is the same as figure 3(*a*) in Llewellyn Smith (with the spurious roots removed). We are interested in the $n = 0$, $\ell < 0$ mode, which exists in all three frequency bands ($\omega > N$, IGW, $\omega < f$) and ceases to be trapped near the shore (i.e. $\xi_c \to \infty$) at $\omega \sim 0.39f$, and wish to investigate how this mode behaves over an arbitrary bottom. This is where the numerical scheme demonstrates its utility, since such an investigation is, in general, impossible by the semianalytic methods of § 2 and laborious by the asymptotic approach of § 4 (since it would require time-consuming calculations to be done repeatedly as the mode is tracked through ω-space). A continuation method is used: a frequency is chosen for which the wave is confined sufficiently close to the shore to resemble the wedge wave function and this is used as the initial guess in the NK scheme to find the wave function in the exponential topography; ω is then decreased and the solution obtained for the previous ω is used to seed the NK scheme for the new ω.

Figure 8(*b*) shows the results. The mode in the exponential basin (Ball's exponential topography with parameters from § 5.1) is found in all three bands, in particular the IGW band, suggesting that edge-trapped IGWs can potentially exist in oceanographic topographies, albeit in this case for non-oceanographic physical parameters. This provides a partial answer to a question that has been the subject of recent debate (Dale & Sherwin 1996; Pringle & Brink 1999; Llewellyn Smith 2004). Interestingly, the mode does not cease to be trapped like its counterpart in the wedge, but the change

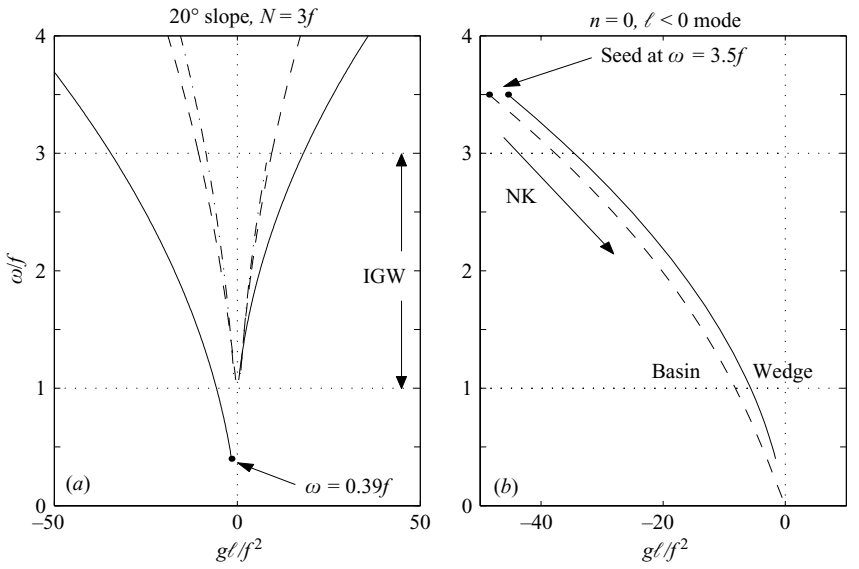

FIGURE 8. (*a*) Dispersion curves for the $n = 0$ (solid line), $n = 1$ (dashed), and $n = 2$ (dot-dash) modes in a 20° wedge with $N = 3f$. The IGW band and the point at which the $n = 0$, $\ell < 0$ mode becomes bottom-trapped are labelled. (*b*) Dispersion curves for the $n = 0$, $\ell < 0$ mode in the wedge (solid line) and Ball's exponential topography (dashed). The seed frequency for the NK continuation scheme is labelled.

in topography appears to stabilize the mode for frequencies lower than $\omega \sim 0.39f$. Figure 9(*a*) shows the wave function in the wedge as ω approaches this critical value. The wave pattern becomes increasingly slanted and confined to the seabed as ω decreases until it eventually sits parallel to the bottom and is no longer trapped. Bottom-trapping such as this is a feature of density stratified flows. Figure 9(*b*) shows the wave function in the exponential basin for the same frequencies. The convex bottom prevents the wave from moving far offshore and the wave remains trapped.

A couple of limiting cases are often employed in the literature so it is worth briefly noting their effect. We consider the Boussinesq approximation ($b = 0$ but non-zero N) and rigid-lid approximation ($\lambda = 0$) numerically. Exhaustive results are not presented here; instead we summarize for the $n = 0$ mode. There are four possibilities: the full equations, Boussinesq, rigid-lid and Boussinesq rigid-lid. In the subinertial band, we find trapping for the full-equation and rigid-lid cases, but not for the Boussinesq and Boussinesq rigid-lid cases (note that the Ou (1980) modes exist for $n > 0$). In the IGW band, we again find clear trapping for the cases full-equation and rigid-lid. The Boussinesq case has oscillations in the interior that are not localized near the edge and is not actually trapped. Neither is the Boussinesq rigid-lid case. Finally for $\omega > N$ both the full-equation and Boussinesq cases trap but there are no modes when the rigid-lid approximation is made. Thus an important point is that the trapped modes we find for the stratified rotating fluid are properly internal modes for $\omega < N$, since they also exist in the case of a rigid lid. Indeed, for the rigid-lid case, the form of (A 9) suggests that trapping is possible in the IGW band, as observed.

5.3. *Oceanographic relevance*

Having established that trapped modes can potentially exist in the IGW band and be reproduced in experiments, we now consider some realistic oceanographic parameters.

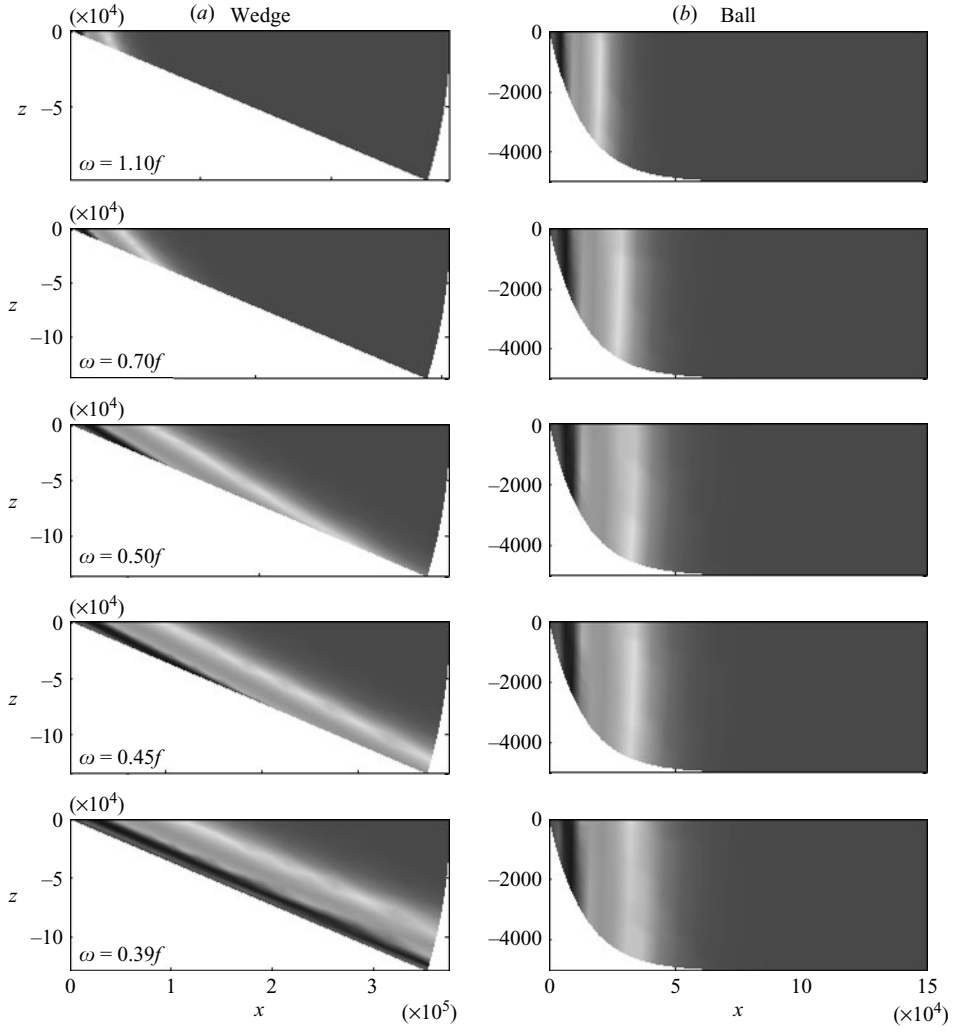

FIGURE 9. Two-dimensional plots of the wave function in the wedge (*a*) and the exponential basin (*b*) as frequency approaches the critical value for bottom-trapping in the wedge. The values of ω are labelled on the plots for the wedge.

We use a representative model of the ocean off the west coast of Oahu, Hawaii: Ball's topography with $H_0 = 4.5 \times 10^3\,\mathrm{m}$ and $a = 7.4 \times 10^{-5}\,\mathrm{m}^{-1}$ such that $\varepsilon = 1/3$; and physical parameters $g = 10\,\mathrm{m\,s}^{-2}$, $f = 1.35 \times 10^{-4}\,\mathrm{s}^{-1}$, and $N = 2f$. Except for the rotation and stratification parameters, this is similar to the previous problem considered.

The lowest two modes propagating in each direction were studied using the NK-continuation method outlined above, seeded with the exact results for a wedge of equal initial slope at sufficiently high frequencies. Table 2 shows the approximate frequencies ω_{min} at which each mode ceases to be trapped near the coast. The modes cease to be trapped well before the frequency reaches the IGW band ($2 < \omega/f < 1$). Repeating the numerical calculation with slightly different parameters suggests that these minimum frequencies are strongly dependent on topography and only weakly

n	Direction	ω_{min} (s^{-1})	ω_{min}/f
0	$\ell > 0$	3.38×10^{-3}	25
0	$\ell < 0$	3.38×10^{-3}	25
1	$\ell > 0$	2.57×10^{-2}	190
1	$\ell < 0$	2.16×10^{-2}	160

TABLE 2. The minimum trapping frequencies for the lowest four modes west off Oahu.

dependent on rotation and stratification. Therefore, whether or not trapped modes exist in the IGW band for a particular topography largely depends on where the IGW band lies with respect to these almost-fixed frequencies. In the previous problem the Coriolis frequency was sufficiently large that the IGW band lay entirely above the minimum frequency. However, it would appear that for realistic rotation and stratification, the band lies well below the minimum frequency, which suggests it may be difficult to find genuine oceanographic scenarios for which trapped IGWs exist.

6. Concluding remarks

Two methods, one numerical and the other asymptotic, have been developed to study stratified rotating-edge waves over a gently sloping bottom of arbitrary topography. The numerical scheme is found to be highly accurate and versatile. Asymptotic solutions are generated using classical WKBJ theory and a long-range uniform theory which corrects for deficiencies in the classical theory at the shoreline, caustic, and for propagation over long ranges. The latter is found to give a much improved wave function but, remarkably, no improvement to the dispersion relation. It is also found that the incorporation of rotation and stratification, previously done using integral-transform methods, can be generated comparatively straightforwardly by classical WKBJ theory. The asymptotics are cross-verified with the numerical method, and compared with the shallow-water approximation and a crude approximation treating the topography as a wedge. Finally, the utility of the methods developed in this paper is demonstrated by an investigation of trapped modes in the IGW frequency band for both laboratory and oceanographic situations.

S. G. L. S. was partially supported by NASA Goddard Grant NAG5-12388. A. T. I. A. thanks the EPSRC for support and R. V. C. thanks the Departments of Mathematics at the Universities of Alberta and British Columbia for their hospitality whilst some of this work was being carried out. We also thank the referees for their helpful comments.

Appendix A. Classical WKBJ approximation with non-zero f and N

Introducing rotation and stratification and retaining the slow variable ξ, the governing equations are

$$s^2\phi_{zz} + \varepsilon^2\phi_{\xi\xi} - (\ell^2 + \sigma^2)\phi = 0, \qquad -h(\xi) < z < 0, \tag{A 1}$$

$$\phi_z - \lambda\phi = 0, \qquad z = 0, \tag{A 2}$$

$$s^2\phi_z - s\sigma\phi - \varepsilon\gamma\ell h'\phi + \varepsilon^2 h'\phi_\xi = 0, \qquad z = -h(\xi), \tag{A 3}$$

where $\sigma = sb/2$ and $\gamma = f/\omega$. The equation hierarchies (4.5)–(4.7) become:

$$\sum_{j=0}^{\infty} \varepsilon^j \left[s^2 A^{(j)}{}_{zz} - (\ell^2 + \sigma^2 - S'^2) A^{(j)} + 2S' A_\xi^{(j-1)} + S'' A^{(j-1)} + A_{\xi\xi}^{(j-2)} \right] = 0, \tag{A 4}$$

$$\sum_{j=0}^{\infty} \varepsilon^j \left[A^{(j)}{}_z - \lambda A^{(j)} \right] = 0, \tag{A 5}$$

$$\sum_{j=0}^{\infty} \varepsilon^j \left[s^2 A^{(j)}{}_z - s\sigma A^{(j)} + (S' - \gamma\ell) h' A^{(j-1)} + h' A_\xi^{(j-2)} \right] = 0. \tag{A 6}$$

Redefining $\kappa = (\ell^2 + \sigma^2 - S'^2)^{1/2}$, the solution satisfying (A 4) and (A 6) for $j = 0$ is $A^{(0)} = a_0(x)\psi(x, z)$, where

$$\psi = N(x) \left\{ \frac{\sigma}{\kappa} \sinh \left[\frac{\kappa}{s}(z + h) \right] + \cosh \left[\frac{\kappa}{s}(z + h) \right] \right\}, \tag{A 7}$$

with normalization constant

$$N(x) = \left[\left(1 - \frac{\sigma^2}{\kappa^2} \right) \frac{h}{2} + \left(1 + \frac{\sigma^2}{\kappa^2} \right) \frac{\sinh(\kappa h/s)\cosh(\kappa h/s)}{2\kappa/s} + \frac{\sigma \sinh^2(\kappa h/s)}{\kappa^2/s} \right]^{-1/2}, \tag{A 8}$$

so that (4.13) holds. Satisfaction of the surface boundary condition (A 5) for $j = 0$ yields the analogue of (4.14):

$$\kappa \tanh(\kappa h/s) = \frac{s\lambda - \sigma}{1 - s\lambda\sigma/\kappa^2}. \tag{A 9}$$

Note that the location of the caustic, $\xi = \xi_c$, given by setting $\kappa = (\ell^2 + \sigma^2)^{1/2}$ in (A 9), is not the same as before.

Multiplying the $j = 1$ equation of (A 4) by $A^{(0)}$, integrating over the depth and applying the boundary conditions on $A^{(0)}$ and $A^{(1)}$, we find that the terms containing σ cancel to leave

$$\frac{(S' - \gamma\ell)h'}{s^2} A^{(0)2}(\xi, -h) = -\frac{(S' a_0^2)'}{s^2} + \frac{S'h'}{s^2} A^{(0)2}(\xi, -h), \tag{A 10}$$

which can be simplified to give the transport equation

$$(S' a_0^2)' - \frac{\gamma\ell\psi^2(\xi, -h)h'}{S'} (S' a_0^2) = 0. \tag{A 11}$$

The solution, up to an arbitrary multiplicative constant, is

$$a_0(\xi) = S'(\xi)^{-1/2} \exp \left[\frac{\gamma\ell}{2} \int^{\xi} \frac{\psi^2(\xi, -h)}{S'(\xi)} h' \, \mathrm{d}\xi \right]. \tag{A 12}$$

Noting that $\psi^2(\xi, -h) = N^2(\xi)$ from (A 7), and that the integral is effectively taken over h, we can write the solution decaying in $\xi > \xi_c$ as

$$\phi = \psi(\xi, z) \left[\ell^2 + \sigma^2 - \kappa^2(\xi) \right]^{-1/4} \exp \left\{ -\frac{1}{\varepsilon} \int_{\xi_c}^{\xi} \left[\ell^2 + \sigma^2 - \kappa^2(\xi) \right]^{1/2} \mathrm{d}\xi + \frac{\gamma\ell}{2} \int_{h_c}^{h} \frac{N^2 \, \mathrm{d}h}{\left(\ell^2 + \sigma^2 - \kappa^2 \right)^{1/2}} \right\}. \tag{A 13}$$

Applying the WKBJ connection formula gives the oscillatory solution in $\xi < \xi_c$:

$$\phi = 2\psi(x,z)\left[\kappa^2(\xi)-\ell^2-\sigma^2\right]^{-1/4}\sin\left\{\frac{1}{\varepsilon}\int_{\xi}^{\xi_c}\left[\kappa^2(\xi)-\ell^2-\sigma^2\right]^{1/2}\,\mathrm{d}\xi - \frac{\gamma\ell}{2}\int_{h}^{h_c}\frac{N^2\,\mathrm{d}h}{\left(\kappa^2-\ell^2-\sigma^2\right)^{1/2}}+\frac{\pi}{4}\right\}. \tag{A 14}$$

The integral constraint can be deduced from the argument of the sine:

$$\frac{1}{\varepsilon}\int_0^{\xi_c}\left[\kappa^2(\xi)-\ell^2-\sigma^2\right]^{1/2}\,\mathrm{d}\xi \sim \left(n+\frac{1}{2}\right)\pi+\frac{\gamma\ell}{2}\int_0^{h_c}\frac{N^2\,\mathrm{d}h}{\left(\kappa^2-\ell^2-\sigma^2\right)^{1/2}}+O(\varepsilon), \tag{A 15}$$

for non-negative integer n. The integral on the right-hand side is evaluated by changing the integration variable from h to κ and eliminating h from N^2 to give

$$\int_{\sqrt{\ell^2+\sigma^2}}^{\infty}\frac{2\kappa\,\mathrm{d}\kappa}{\left(\kappa^2-\sigma^2\right)\left(\kappa^2-\ell^2-\sigma^2\right)^{1/2}}=\frac{\pi}{|\ell|}, \tag{A 16}$$

which is found by complex integration around a large circle with two keyhole contours for the branch cuts emanating from $\kappa = \pm\sqrt{\ell^2+\sigma^2}$. The integral constraint becomes

$$\frac{1}{\varepsilon}\int_0^{\xi_c}\left[\kappa^2(\xi)-\ell^2-\sigma^2\right]^{1/2}\,\mathrm{d}\xi \sim \left(n+\frac{1}{2}+\frac{\gamma\,\mathrm{sgn}\,\ell}{2}\right)\pi+O(\varepsilon), \tag{A 17}$$

which agrees with the result previously obtained using Whitham's (1979) integral transform techniques (Zhevandrov 1991; Sun & Shen 1994; Llewellyn Smith 2004).

Appendix B. Eigenvalues of Zhevandrov's comparison equation

Zhevandrov's comparison equation, defined by (4.30) and (4.33), can be written in a form independent of ε by setting $\rho = \varepsilon\zeta$:

$$\zeta V_{\zeta\zeta}+V_{\zeta}+(\zeta_c-\zeta)V=0. \tag{B 1}$$

V is regular at $\zeta = 0$ and ζ_c, and decays as $\zeta\to\infty$. The decay condition suggests it may bear fruit to write $V = \mathrm{e}^{-\mu\zeta}W(\zeta)$, where μ is to be determined, whence

$$\zeta W_{\zeta\zeta}+(1-2\mu\zeta)W_{\zeta}+\left[(\mu^2-1)\zeta+(\zeta_c-\mu)\right]W=0. \tag{B 2}$$

We can put this into the form of Kummer's equation (see Abramowitz & Stegun 1974, § 13.1.1) by setting $\mu = 1$ and changing the independent variable to $\eta = 2\zeta$:

$$\eta W_{\eta\eta}+(1-\eta)W_{\eta}-\left(\frac{1-\zeta_c}{2}\right)W=0. \tag{B 3}$$

The solution regular at $\eta = 0$ is

$$W(\eta)=M\left(\frac{1-\zeta_c}{2},1,\eta\right), \tag{B 4}$$

where M is the confluent hypergeometric function. Returning to $V(\zeta)$ and examining the large-ζ limit (Abramowitz & Stegun 1974, § 13.1.4), we have

$$V(\zeta)=\mathrm{e}^{-\zeta}M\left(\frac{1-\zeta_c}{2},1,2\zeta\right)\sim\mathrm{e}^{\zeta}\frac{\Gamma(1)}{\Gamma[(1-\zeta_c)/2]}(2\zeta)^{-(1+\zeta_c)/2}\left[1+O(\zeta^{-1})\right] \tag{B 5}$$

as $\zeta \to \infty$. To avoid divergence due to the presence of e^{ζ}, the Gamma function in the denominator must be singular, so its argument must be a non-positive integer:

$$\frac{1-\zeta_c}{2} = -n \quad \to \quad \zeta_c = 2n+1, \quad n = 0, 1, \ldots. \tag{B 6}$$

Finally, $\rho_c = \varepsilon\zeta_c = (2n+1)\varepsilon$, which is the required result.

REFERENCES

Abramowitz, M. & Stegun, I. A. (Ed.) 1974 *Handbook of Mathematical Functions*. Dover.

Adamou, A. T. I., Gridin, D. & Craster, R. V. 2005 Acoustic quasi-modes in slowly-varying cylindrical tubes. *Q. J. Mech. Appl. Maths* **58**, 419–438.

Ball, F. K. 1967 Edge waves in an ocean of finite depth. *Deep-Sea Res.* **14**, 79–88.

Bender, C. M. & Orszag, S. A. 1978 *Advanced Mathematical Methods for Scientists and Engineers*. McGraw-Hill.

Boyd, J. P. 2001 *Chebyshev and Fourier Spectral Methods*, 2nd edn. Dover.

Dale, A. C. & Sherwin, T. J. 1996 The extension of baroclinic coastal-trapped wave theory to superinertial frequencies. *J. Phys. Oceanogr.* **26**, 2305–2315.

Davies, E. B. & Parnovski, L. 1998 Trapped modes in acoustic waveguides. *Q. J. Mech. Appl. Maths* **51**, 477–492.

Duclos, P. & Exner, P. 1995 Curvature-induced bound states in quantum waveguides in two and three dimensions. *Rev. Maths Phys.* **7**, 73–102.

Evans, D. V. 1988 Mechanisms for the generation of edge waves over a sloping beach. *J. Fluid Mech.* **186**, 379–391.

Evans, D. V. 1989 Edge waves over a sloping beach. *Q. J. Mech. Appl. Maths* **42**, 131–142.

Evans, D. V., Levitin, M. & Vassiliev, D. 1994 Existence theorems for trapped modes. *J. Fluid Mech.* **261**, 21–31.

Greenspan, H. P. 1970 A note on edge waves in a stratified fluid. *Stud. Appl. Maths* **49**, 381–388.

Gridin, D., Adamou, A. T. I. & Craster, R. V. 2004 Electronic eigenstates in quantum rings: Asymptotics and numerics. *Phys. Rev.* B **69**, 155317.

Gridin, D., Adamou, A. T. I. & Craster, R. V. 2005*a* Trapped modes in curved elastic plates. *Proc. R. Soc. Lond.* A **461**, 1181–1197.

Gridin, D., Craster, R. V. & Adamou, A. T. I. 2005*b* Trapped modes in bent elastic rods. *Wave Motion* **42**, 352–366.

Kaplunov, J. D., Rogerson, G. A. & Tovstik, P. E. 2005 Localized vibration in elastic structures with slowly varying thickness. *Q. J. Mech. Appl. Maths* **58**, 645–664.

Kravtsov, Y. A. 1964 A modification of the geometrical optics method. *Radiofizika* **7**, 664–673, in Russian.

Langer, R. E. 1931 On the asymptotic solutions of ordinary differential equations with an application to the Bessel functions of large order. *Trans. Am. Maths Soc.* **33**, 23–64.

Linton, C. & Ratcliffe, K. 2004 Bound states in coupled guides. I. Two dimensions. *J. Maths Phys.* **45**, 1359–1379.

Llewellyn Smith, S. G. 2004 Stratified rotating edge waves. *J. Fluid Mech.* **498**, 161–170.

Ludwig, D. 1966 Uniform asymptotic expansions at a caustic. *Comm. Pure Appl. Maths* **19**, 215–250.

McIver, M. 1999 Uniqueness below a cut-off frequency for the two-dimensional linear water-wave problem. *Proc. R. Soc. Lond.* A **455**, 1435–1441.

McKee, W. D. 1973 Internal-inertia waves in a fluid of variable depth. *Proc. Camb. Phil. Soc.* **73**, 205–213.

Miles, J. 1989 Edge waves on a gently sloping beach. *J. Fluid Mech.* **199**, 125–131.

Munk, W. H., Snodgrass, F. & Wimbush, M. 1970 Tides off shore: Transition from California coastal to deep-sea waters. *Geophys. Fluid Dyn.* **1**, 161–235.

Muzylev, S. V., Bulgakov, S. N. & Duran-Matute, M. 2005 Edge capillary-gravity waves on a sloping beach. *Phys. Fluids* **17**, 048103.

Muzylev, S. V. & Odulo, A. B. 1980 Waves in a rotating stratified fluid on a sloping beach. *Dokl. Akad. Nauk. SSSR* **250**, 331–335.

Ou, H. W. 1980 On the propagation of free topographic Rossby waves near continental margins. I. Analytic model for a wedge. *J. Phys. Oceanogr.* **10**, 1051–1060.

Pedlosky, J. 1987 *Geophysical Fluid Dynamics*, 2nd edn. Springer.

Pringle, J. M. & Brink, K. H. 1999 High-frequency internal waves on a sloping shelf. *J. Geophys. Res.* **104**, 5283–5299.

Saint-Guily, B. 1968 Ondes de frontière dans un bassin tournant dont le fond est incliné. *C. R. Acad. Sci. Paris* **266**, 1291–1293.

Shen, M. C. & Keller, J. B. 1975 Uniform ray theory of surface, internal and acoustic wave propagation in a rotating ocean or atmosphere. *SIAM J. Appl. Maths* **28**, 857–875.

Shen, M. C., Meyer, R. E. & Keller, J. B. 1968 Spectra of water waves in channels and around islands. *Phys. Fluids* **11**, 2289–2304.

Smith, R. 1977 Propagation in slowly-varying wave-guides. *SIAM J. Appl. Maths* **33**, 39–50.

Stokes, G. G. 1846 Report on recent researches in hydrodynamics. *Brit. Ass. Rep.* **1**, 1–20.

Sun, S. M. & Shen, M. C. 1994 Linear water waves over a gently sloping beach. *Q. J. Appl. Maths* **52**, 243–259.

Ursell, F. 1952 Edge waves on a sloping beach. *Proc. R. Soc. Lond.* A **214**, 79–97.

Whitham, G. B. 1979 *Lectures on Wave Propagation, Tata Institute of Fundamental Research Lectures on Mathematics and Physics*, vol. 61. New Delhi: Narosa.

Zhevandrov, P. 1991 Edge waves on a gently sloping beach: uniform asymptotics. *J. Fluid Mech.* **233**, 483–493.